

# Effect of soil resistance on the low strain mobility response of piles using impulse transient response method

Liang, L. & Beim, J.

*Pile Dynamics, Inc., Cleveland, Ohio, U.S.A.*

Keywords: low strain, mobility, soil resistance, ITR, pile integrity

**ABSTRACT:** The impulse transient response method has been introduced to pile integrity testing over thirty years ago. The main premise of this method is to measure both pile top velocity and force induced at the pile top by a small hammer impact. The measured velocity may be considered the response to the force input. The force and velocity records are examined to determine either the integrity or the length of the pile based on a known or assumed wave speed. In general, only the velocity vs. time signal has been widely used in the interpretation because of its direct relationship to the physical pile conditions and therefore relative ease of interpretation. There are several disadvantages of solely using velocity vs. time, which include: 1) the judgment is based on visual examination instead of quantitative analysis and thus the experience of the testers play crucial role in making a correct assessment and 2) the force information which can help to determine the pile condition near the top and the strength of the pile/soil system is ignored.

Recent developments in both equipment and software make measurements and the calculation of the mobility in the frequency domain much faster and more accurate. To take advantage of the force measurement, it is necessary to better understand the frequency response of piles embedded in soil.

This paper presents studies of the effect of soil resistance distribution on the mobility. Numerically simulated velocity and force curves of an impact applied to pile top for different soil resistance distributions were generated. These curves were then subjected to Fourier analysis yielding the mobility spectrum and dynamic stiffness. The relationship between pile non-uniformities, soil resistance distribution, mobility spectrum and dynamic stiffness was then investigated, aiming at developing a guideline for data interpretation based on mobility spectra. Mobility spectra obtained from data collected on real piles are also presented for comparison.

## 1 INTRODUCTION

Due to its low cost, easy use and no need of advanced planning, the dynamic low-strain method is the most frequently used Non Destructive Test (NDT) method for assessing the structural integrity of concrete driven piles, cast-in-place piles, concrete filled steel pipe piles and timber piles. It is accomplished by hitting the top of the pile or shaft with a light hand-held hammer, and recording the ensuing top motion with a high sensitivity accelerometer (Rausche et al, 1992). Sometimes an instrumented hammer is used, allowing the recording also of the impact force. There are basically two ways of interpreting the data collected by these devices: the Pulse Echo Method (PEM), and the Impulse Transient Response Method (ITRM or TRM) (Rausche, 2004). The PEM uses the velocity signal obtained by integration of the acceleration data. The analysis is done in the time domain, by detecting the effects of the reflections of the low-strain compression

wave when it encounters changes in the impedance  $Z$ , given by the expression:

$$Z = \frac{EA}{c} = A\sqrt{E\rho} \quad (1)$$

In which  $A$  is the cross-section area,  $E$  is the elastic modulus,  $c$  is the wave speed and  $\rho$  is the mass density of the pile material.

Since the soil resistance also causes reflections of the wave, its effect has to be eliminated by filters or considered in the analysis. The applied force record, if available, can be used to help detect impedance changes close to the pile top.

The TRM analyzes both the velocity and the force signals in the frequency domain. This can be easily accomplished on modern PC's using Fast Fourier Transform (FFT). Its concept is similar to the Vibration Method (VM) (Davis and Dunn 1974), where a vibrator is placed on top of the pile and its frequency is varied over a certain range. In the case of

TRM the variable frequency excitation is produced by the hammer blow, whose spectrum contains all frequencies from zero to the maximum usually used with VM. The velocity spectrum is divided by the force spectrum to determine the Mobility or Mechanical Admittance spectrum. This spectrum is then analyzed for peaks corresponding to resonant frequencies.

For a pile of length  $L$  and wave speed  $c$ , laterally unrestrained and resting on top of elastic soil, the resonant frequencies will be equally spaced at intervals  $\Delta f$  equal to:

$$\Delta f = \frac{c}{2L} \quad (2)$$

According to Davis and Dunn (1974), in the case of a laterally unrestrained pile resting on an infinitely rigid base the lowest frequency of resonance has a value of  $c/4L$ . On the other hand, if a laterally unrestrained pile rests on an infinitely compressible base, resonance first occurs at a very low frequency. For laterally unrestrained piles resting on soils of normal elasticity and compressibility the lowest frequency of resonance will be in an intermediate position between this very low value and  $c/4L$ , as shown in Fig. 1.

Fig. 1 shows that a rigidly supported pile has a low mobility and a free pile has a high mobility at the origin. It is therefore expected that the slope of the line in the beginning of the curve could indicate the type of base or toe resistance. In fact, the inverse of the slope of this straight line is the so-called Dynamic Stiffness, which has been used as an indication of the combined pile-soil stiffness.

There are two numerical results that are usually determined from the plot shown in Fig. 1. One is the already mentioned Dynamic Stiffness (DS), which can be defined as:

$$DS = \frac{2\Pi f_m}{M} \quad (3)$$

In which  $M$  is the mobility at frequency  $f_m$ . The other numerical result usually used is the average or

characteristic value of the Mobility  $N$ , which is given by:

$$N = \frac{1}{Z} = \sqrt{PQ} \quad (4)$$

In which  $P$  is the maximum and  $Q$  is the minimum Mobility value within the frequency range analyzed (excluding the first resonant peak). If  $N$  is normalized in terms of the inverse of the pile top impedance  $1/Z$ , a value greater than 1 could mean a pile with impedance reductions along the shaft, which could mean a reduction in any of the terms on equation (1). A value of  $N$  smaller than 1 on the other hand could mean a pile with impedance increases along the shaft.

Therefore,  $DS$  given in expression (3) can be seen as a relative measure of the combined stiffness of the pile and soil, while  $N$  given in expression (4) should give a number relating to the pile shape.

## 2 COMPUTER SIMULATIONS – FIXED PILE GEOMETRY

A one-dimensional wave propagation simulation computer program was used to realistically simulate the force-velocity signal for different soil configurations. The program simulates a fixed half sine force excitation with a maximum value of 5 kN (1,120 lbs) and duration of 1 ms, within the range of values usually encountered in Low Strain tests, and uses the Smith (Smith, 1960) approach to calculate the resulting velocity at the top of a uniform cylindrical pile, with 500 mm (19.7 inches) diameter and 10 m (32.8 ft) length, embedded in soils of different static resistances and damping factors. A constant quake of 2.54 mm (0.1 inch) was used for the soil along the shaft, and a quake of 4.17 mm (0.16 inch), corresponding to the diameter divided by 120 ( $D/120$ ), was used at the toe. A wave propagation speed of 4000 m/s (13123 ft/sec) and specific weight of 24 kN/m<sup>3</sup> (153 lbs/ft<sup>3</sup>) were used for the pile material. The spectra of the applied force and of the resulting velocity were then determined using standard FFT routines, and the ratios of the velocity amplitudes with respect to the force amplitudes, normalized with respect to the mechanical admittance ( $1/Z$ ) of the pile were plotted against frequency.

In the first series of simulations, a cohesive soil (skin Smith damping equal to 0.65 s/m or 0.2 s/ft) with a triangular distribution starting with a low resistance at the top was considered. To analyze the effect of total resistance and resistance distribution, first a low ultimate static soil resistance of 500 kN (112 kips) and then a high (for this size pile) ultimate resistance of 5000 kN (1120 kips) were analyzed. Two simulations were made for each capacity, one with an end bearing of 20% of the total resistance, and

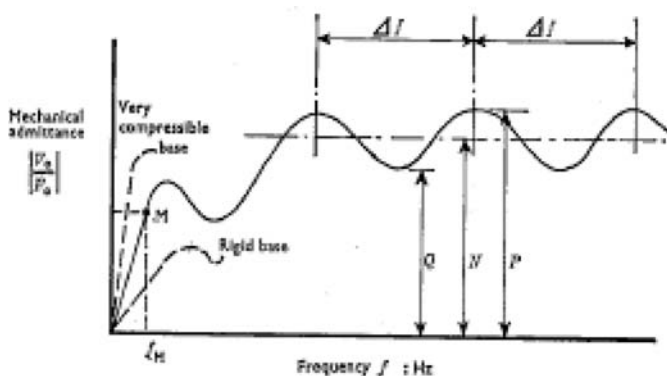


Figure 1. Response curve for cylindrical pile (Davis and Dunn, 1974).

the second with an end bearing of 90% of the total resistance. The results are shown in Figs. 2a to 2d below, shown in order of increasing skin friction.

The results indicate that the lowest frequency of resonance and the Dynamic Stiffness increase as the skin friction increases. The lowest frequency of resonance approaches  $c/4L$  (corresponding to 100 Hz in this case) for a skin friction of 4000 kN (900 kips).

The maximum normalized peak after the lowest frequency of resonance (P) seems to be related to the total resistance. Higher values of P correspond to lower total resistances.

The normalized characteristic mobility value (square root of P times Q) seems to be independent of the soil resistance. For the uniform piles simulated these values were close to one, i.e., the values of the characteristic mobility were close to  $1/Z$ .

In order to have an idea of the effect of soil type on the mobility spectrum, simulations corresponding to the resistance distribution of Figs. 2c and 2d were

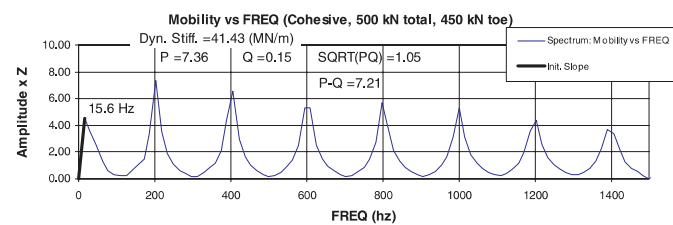


Figure 2a. Simulated Mobility spectrum, cohesive soil with 500 kN total resistance and 90% end bearing.

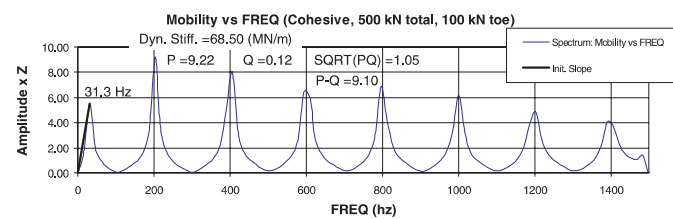


Figure 2b. Simulated Mobility spectrum, cohesive soil with 500 kN total resistance and 20% end bearing.

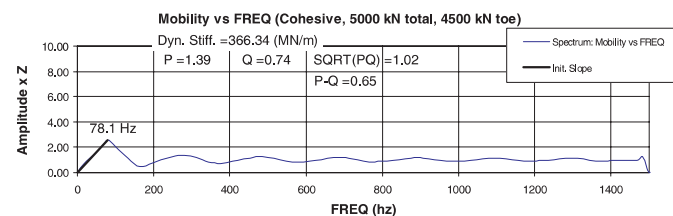


Figure 2c. Simulated Mobility spectrum, cohesive soil with 5000 kN total resistance and 90% end bearing.

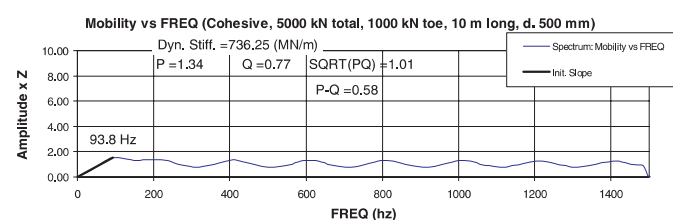


Figure 2d. Simulated Mobility spectrum, cohesive soil with 5000 kN total resistance and 20% end bearing.

made, but with a skin Smith damping factor of 0.16 s/m (0.05 s/ft), corresponding to non-cohesive soil. The resulting simulations are shown in Figs. 3a and 3b.

Interestingly, the lowest frequency of resonance did not change with a lower damping factor, so it seems that this frequency is more related to static resistance. However, the Dynamic Stiffness was reduced and the P value increased in relation to the values on Figs. 2c and 2d, which should be expected due to the lower total (static plus dynamic) resistance with the lower damping factor.

In order to verify the effect of end bearing on the mobility spectrum, another series of simulations were made with constant skin friction equal to 1000 kN (225 kips), and end bearing increasing from 500 kN (112 kips) to 4000 kN (900 kips). The results are shown in Figs. 4a to 4c, in order of increasing end bearing.

The results seem to indicate that for constant skin friction the lowest resonant frequency and the

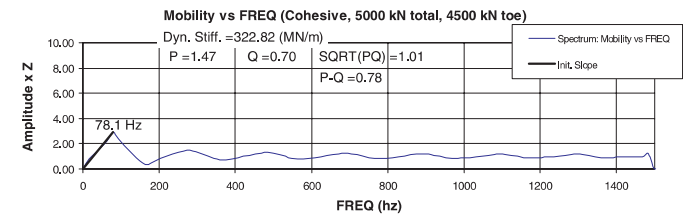


Figure 3a. Mobility spectrum, non-cohesive soil with 5000 kN total resistance and 90% end bearing.

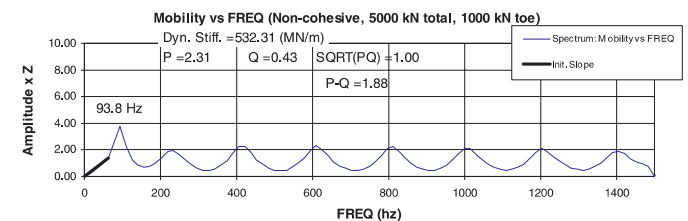


Figure 3b. Mobility spectrum, non-cohesive soil with 5000 kN total resistance and 20% end bearing.

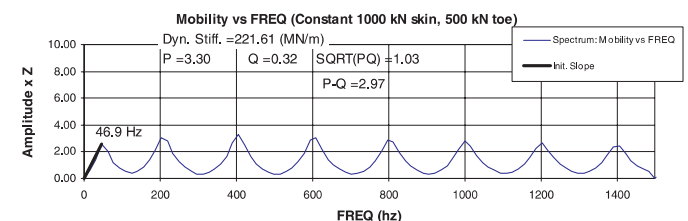


Figure 4a. Simulated Mobility spectrum, cohesive soil with 1000 kN skin friction and 500 kN end bearing.

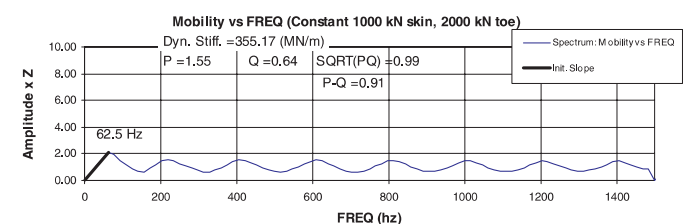


Figure 4b. Simulated Mobility spectrum, cohesive soil with 1000 kN skin friction and 2000 kN end bearing.

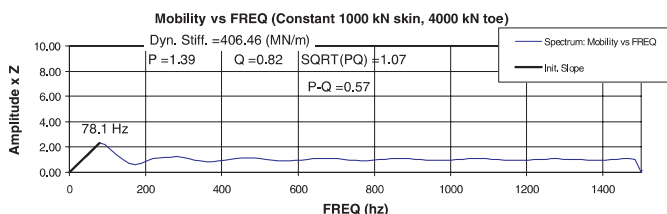


Figure 4c. Simulated Mobility spectrum, cohesive soil with 1000 kN skin friction and 4000 kN end bearing.

Dynamic Stiffness increase as end bearing increases. An inverse relationship between P and P-Q with end bearing also seems to exist.

### 3 COMPUTER SIMULATIONS – VARIABLE PILE GEOMETRY

In the above simulations only variations in the characteristics of the soil were considered. Changes in the geometry of the pile also affect the mobility spectrum, and this fact can be used for helping diagnose defects in the pile (Davis and Dunn, 1974). It is not the purpose of this paper to study the effects of pile defects on the mobility spectrum, but some additional simulations were made to show the effects of some frequently found changes in the pile geometry.

In this case the characteristics of the soil were made similar to those of the simulation shown in Fig. 2d above, and were kept unchanged. For comparison purposes this simulation is repeated in Fig. 5a below. Fig. 5b shows the mobility spectrum of a pile with the same diameter but with an increased length of 20 m (65.5 ft), twice that of the original pile. Fig. 5c shows the results for a pile with the same length, but with a reduced diameter of 400 mm (15.7 inch) instead of the original 500 mm. In this case the soil resistance was changed proportionally to the change in shaft perimeter and toe area, thus assuming unchanged soil unit friction and end bearing (the toe quake was also changed, keeping it equal to  $D/120$ ). Fig. 5d shows the results for a pile with the same length as the original one, but with a diameter that tapers down from 500 mm at the top to 400 mm at the pile toe, and Fig. 5e shows the result of a pile with the same length and top diameter as the original one, but with a diameter which increases linearly from the original 500 mm to 600 mm (23.6 inch) over the last 1 m (3.3 feet) length.

The effects of a longer pile shown in Fig. 5b are predictable: the lowest frequency of resonance drops to slightly more than half of its original value and so does the Dynamic Stiffness (due to doubling of the pile length and also due to the reduction in unit skin friction, since the soil resistance was kept constant).

As expected, a smaller overall pile diameter (but with the same soil unit skin friction and end bearing) causes a reduction in the Dynamic Stiffness, as shown in Fig. 5c. Somewhat unexpected, however, is an increase in the lowest frequency of resonance,

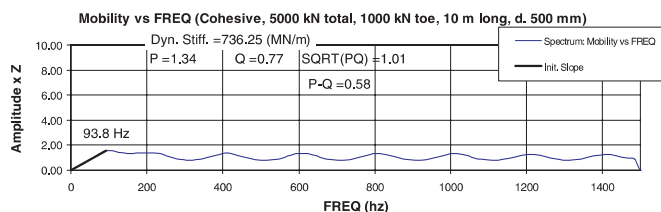


Figure 5a. Simulated Mobility spectrum, cohesive soil with 5000 kN total resistance and 20% end bearing, 10 m long cylindrical pile with 500 mm diameter (repeated from Figure 2d).

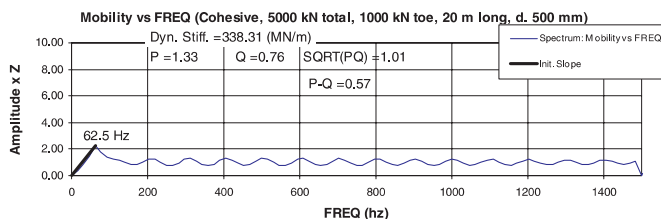


Figure 5b. Simulated Mobility spectrum, cohesive soil with 5000 kN total resistance and 20% end bearing, 20 m long cylindrical pile with 500 mm diameter.

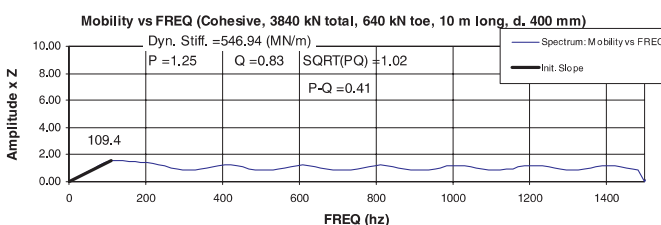


Figure 5c. Simulated Mobility spectrum, cohesive soil with 3840 kN total resistance and 640 kN end bearing, 10 m long cylindrical pile with 400 mm diameter.

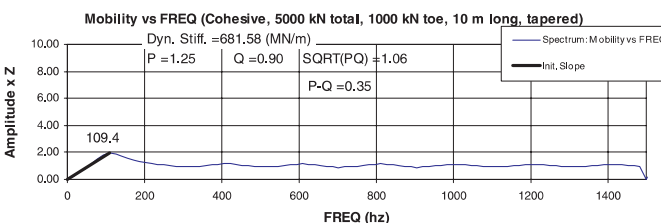


Figure 5d. Simulated Mobility spectrum, cohesive soil with 5000 kN total resistance and 20% end bearing, 10 m long cylindrical pile with 500 mm top and 400 mm bottom diameter.

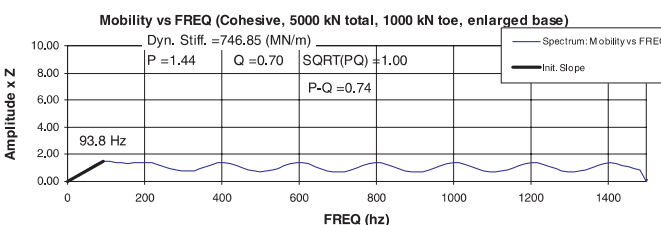


Figure 5e. Simulated Mobility spectrum, cohesive soil with 5000 kN total resistance and 20% end bearing, 10 m long cylindrical pile with 500 mm top and linear increase to 600 mm diameter from 9 m to 10 m.

which in this case is reaching the laterally unrestrained fixed base pile value of 100 Hz.

The results for the tapered pile shown in Fig. 5d are similar to those for the 400 mm diameter pile, except that the Dynamic Stiffness is larger, as expected. It should be noted that by keeping the same original

values for the skin friction and end bearing, even though the perimeter and toe area are now smaller, this simulation is actually assuming a slightly larger unit skin friction and end bearing. This may explain the higher value of the lowest frequency of resonance.

Finally, the simulation for the enlarged base pile shown in Fig. 5e is showing a slightly larger Dynamic Stiffness than the original one shown in Fig. 5a, as expected. The lowest resonant frequency is the same.

#### 4 REAL WORLD PROBLEMS

Systematic actual field tests to confirm the effects of the soil in the Mobility plot were not made; it may be an interesting matter for further investigation. However, one of the problems often encountered in real practice with low strain integrity testing was investigated, namely, the sensitivity of the method to the differences which might exist between different records taken on the same pile. Figs. 6a to 6c below show three force-velocity records of the same 254 mm × 254 mm (10'' × 10'') precast concrete pile, 12.2 m (40') long, which was lying on top of a man-deposited clay fill. The pile was hit on one

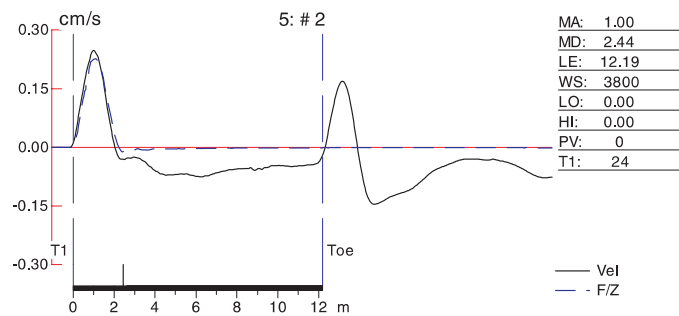


Figure 6a. Force-velocity record of signal #2.

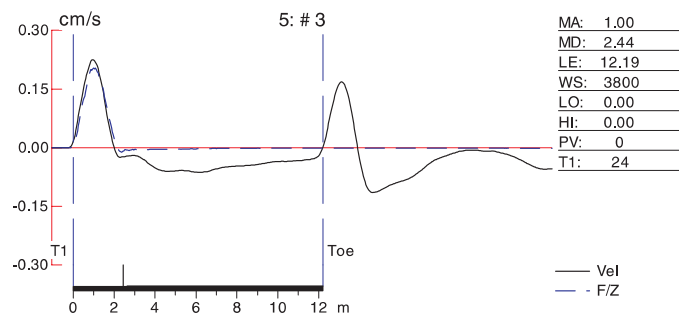


Figure 6b. Force-velocity record of signal #3.

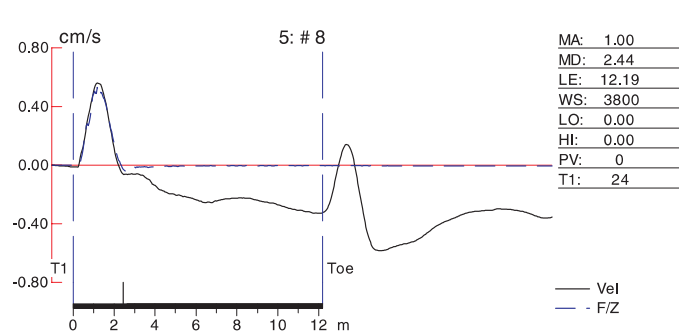


Figure 6c. Force-velocity record of signal #8.

side with a 900 g (2 lbs) hammer, and the other side was free. Each signal is the average of five blows, and is shown without any filtering or other kind of enhancement.

The signal in Fig. 6c has a clear negative drift which is absent in the other two. Although in this case it would have been advisable to discard this record and work only with the other two, in real practice many times one is left with only one reasonably acceptable record to analyze. A signal like the one shown in Fig. 6c could be interpreted as corresponding to a pile with a high amount of skin friction, when in fact the negative drift can have other causes, like loose or lower quality material at the pile top, for example.

Figs. 7a to 7c below show the Mobility spectra corresponding to the signals of Figs. 6a to 6c.

As it can be seen, all spectra are showing the same lowest resonant frequency of 21.3 Hz, much below the fixed pile limit of 77.9 Hz ( $c/4L$ ), as expected due to the near absence of any soil resistance. The values for P and P-Q are very similar (3.631, 3.708, 3.684 and

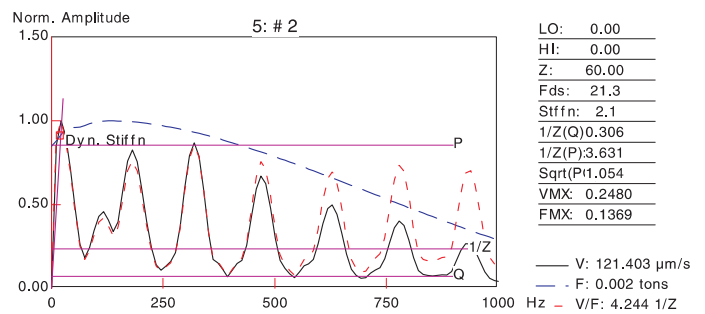


Figure 7a. Velocity (solid black), Force (dashed blue) and Mobility (dashed red) spectra of record for blow #2.

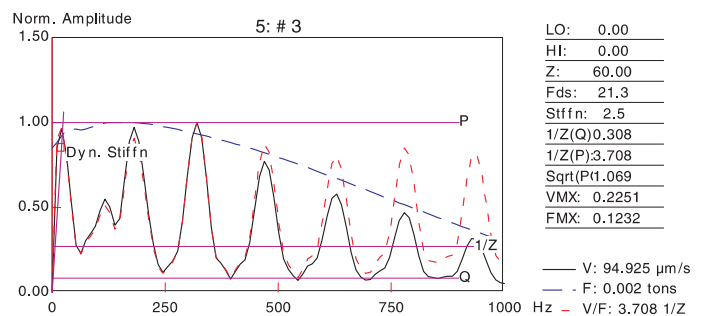


Figure 7b. Velocity (solid black), Force (dashed blue) and Mobility (dashed red) spectra of record for blow #3.

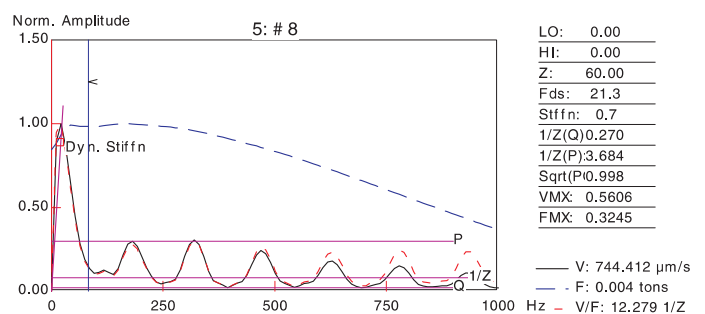


Figure 7c. Velocity (solid black), Force (dashed blue) and Mobility (dashed red) spectra of record for blow #8.

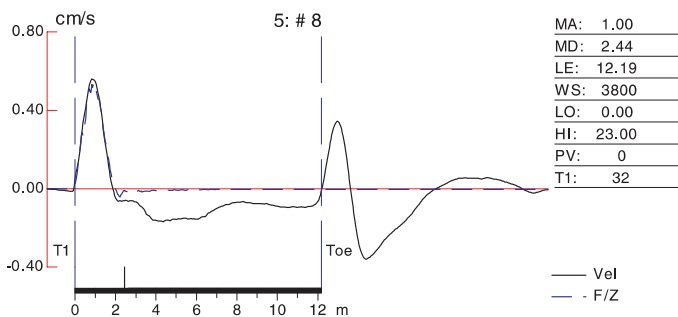


Figure 8a. Filtered force-velocity plot record for blow #8.

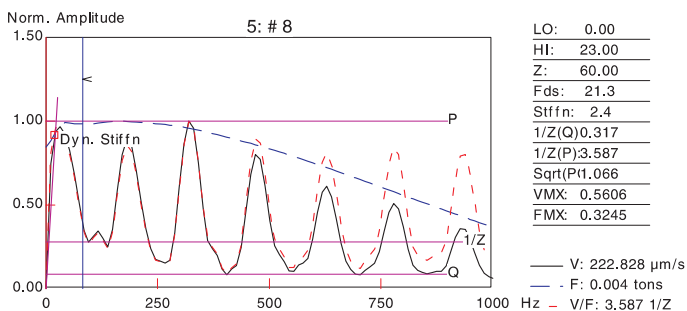


Figure 8b. Velocity (solid black), Force (dashed blue) and Mobility (dashed red) spectra of record for blow #8 after hi-pass filtering.

3.325, 3.400, 3.414, respectively), as are the values of the square root of PQ. However, the Dynamic Stiffness in Fig. 7c is about one third of those in Figs. 7a and 7b.

The use of high-pass filter with a cutoff frequency of 82.6 Hz (equivalent to a length of 23 m for a wave speed of 3800 m/s) brings down the amplitude of the first resonant peak, resulting in the signals in the time domain and in the frequency domain shown in Figs. 8a and 8b, respectively.

As it can be seen, the high pass filtering resulted in about the same Dynamic Stiffness as the other two records, with only small changes in the values of P, P-Q and square root of PQ. This could in fact be a good method for determining the right amount of filtering necessary for a given record, without having to rely solely on subjective visual inspection.

## 5 CONCLUSIONS

The effects of the characteristics of surrounding soil on the Mobility spectrum were analyzed. The results are summarized in Table 1.

The following general conclusions were reached:

As suggested by others, a direct relationship between the lowest frequency of resonance and Dynamic Stiffness with skin friction seems to exist.

The value of the maximum peak after the lowest frequency of resonance (P) seems to be inversely related to the total resistance, if other soil parameters such as damping factors and quakes are constant.

For constant skin friction there seems to exist a direct relationship between the lowest resonant frequency and Dynamic Stiffness with end bearing. An inverse relationship between P and P-Q with end bearing also seems to exist.

The Dynamic Stiffness is reduced and the P value increases when changing from cohesive to non-cohesive soils with similar static resistance distribution.

The value of the square root of PQ is relatively independent on the characteristics of the soil.

Table 1. Summary of Simulation Results (Except for indicated in the table, shaft size: Length = 10 m and Diameter = 500 mm)

Figure No.	$R_{total}$ (kN)	$R_{skin}$ (kN)	$R_{toe}$ (kN)	$R_{toe}/R_{total}$ (%)	$D_{skin}$ (s/m)	P 1/Z	Q 1/Z	P-Q 1/Z	N = PQ 1/Z	Dynamic Stiffness (MN/m)	First Resonance Frequency (Hz)	Shaft Geometry	Comment
2a	500	50	450	90%	0.65	7.36	0.15	7.21	1.05	41.4	15.6	Uniform	
2b	500	400	100	20%	0.65	9.22	0.12	9.1	1.05	68.5	31.3	Uniform	
2c	5000	500	4500	90%	0.65	1.39	0.74	0.65	1.01	366.3	78.1	Uniform	
2d	5000	4000	1000	20%	0.65	1.34	0.77	0.57	1.02	736.3	93.8	Uniform	
Effect of Skin Damping Factor													
3a	5000	500	4500	90%	0.16	1.47	0.7	0.77	1.01	322.8	78.1	Uniform	
3b	5000	4000	1000	20%	0.16	2.31	0.43	1.88	1.00	532.3	93.8	Uniform	
Effect of Toe Resistance													
4a	1500	1000	500	33%	0.65	3.3	0.32	2.98	1.03	221.6	46.9	Uniform	
4b	3000	1000	2000	67%	0.65	1.55	0.64	0.91	1.00	355.2	62.5	Uniform	
4c	5000	1000	4000	80%	0.65	1.39	0.82	0.57	1.07	406.5	78.1	Uniform	
Effect of Pile Geometry													
5a	5000	4000	1000	20%	0.65	1.34	0.77	0.57	1.02	736.3	93.8	Uniform	= Figure 2d
5b	5000	4000	1000	20%	0.65	1.33	0.76	0.57	1.01	338.3	62.5	Uniform	L = 20 m
5c	3840	3200	640	17%	0.65	1.25	0.83	0.42	1.02	546.9	109.4	Uniform	D = 400 mm
5d	5000	4000	1000	20%	0.65	1.25	0.9	0.35	1.06	681.6	109.4	Tapered	D: 500 to 400 mm
5e	5000	4000	1000	20%	0.65	1.44	0.7	0.74	1.00	747.0	93.8	D: Linear increase from 500 to 600 mm from 9 to 10 m	

The Dynamic Stiffness is influenced by the amount of high-pass filtering used.

It should be noted that direct measurement of soil resistance or any other soil parameter is not the objective of low strain integrity testing. Therefore, no attempt has been made to determine possible mathematical expressions relating soil resistance as a function of any of the parameters from the Mobility spectrum. The objective of this paper was to show that frequency domain analysis of low strain integrity test data can provide useful comparison information about soil characteristics of piles with the same geometry. Due to the simplicity and quickness of low strain integrity testing, this could be a useful tool for determining which piles should be subjected to high strain or static load test, for instance on a quality control program.

## REFERENCES

- Davis, A.G. and Dunn, C.S., (1994). "From Theory to Field Experience with the Non-destructive Vibration Testing of Piles", Proc. Instn. Civ. Engrs. Part 2, 57, December, 571-593.
- Rausche, F. (2004). Non-Destructive Evaluation Of Deep Foundations. Proceedings of the Fifth International Conference on Case Histories in Geotechnical Engineering: New York, NY; 1-9.
- Rausche, F., Likins, G. E. and Ren-Kung, S. (1992). "Pile integrity testing and analysis". Proceedings of the Fourth International Conference on the Application of Stress-Wave Theory to Piles: The Netherlands; 613-617.
- Smith, E.A.L. (1960). "Pile Driving Analysis by the Wave Equation", ASCE, Journal of Soil Mechanics and Foundations Division, Vol. 86, SM4, Paper No. 2574.

# Stress Wave

Lisbon | 2008



The 8th International  
Conference on the  
**Application of  
Stress Wave  
Theory to Piles**

**Science, Technology  
and Practice**

J.A. Santos  
Editor